P.K. Sinha, et. al. International Journal of Engineering Research and Applications
www.ijera.com
ISSN: 2248-9622, Vol. 12, Issue 6, (Series-V) June 2022, pp. 27-36

RESEARCH ARTICLE OPEN ACCESS

Calibration of a Seven-hole Pressure probe in non-null technique

P.K. Sinha[a], S K Shahi[c], D. Chowdhury[b] and B. Majumdar[b]
[a] *Department of Mechanical Engineering, JLD Engineering and Management College, Baruipur, India*
[b]*Department of Power Engineering, Jadavpur University, Kolkata, India*
[c] *Scientist C, MNRE, Govt. of India, New Delhi*

ABSTRACT
The analysis of fluid flow is encountered in almost all engineering applications. Flow measurements, particularly velocity and its direction, turbulence quantities are needed in order to improve the understanding of various complex flow phenomena and to validate and further refine the computer flow models. Pressure probes find wide application in the measurement of fluid flows both in the laboratory and in the industry. A seven-hole pressure probe is calibrated in non-null technique. An algorithm for seven-hole probe in non-null method is developed which utilizes a database of calibration data and a local least-squares interpolation technique is used for interpolation of flow properties. It is also found out that the non-null method was superior in ease of use and prediction of flow measurement variables.
Keywords: seven-hole probe, non-null method, interpolation technique, regression model, sector scheme.

Date of Submission: 13-06-2022 Date of Acceptance: 27-06-2022

Nomenclature

C_{α}	Pitch angle coefficient
C_{β}	Yaw angle coefficient
$f_1, f_2, f_3, F(\alpha), k$	Calibration constants
G	Acceleration due to gravity(m/s^2)
U	Mean velocity (m/sec)
U_X	Velocity in x-direction (m/sec)
U_Y	Velocity in y-direction (m/sec)
U_Z	Velocity in z-direction (m/sec)
C_{Ptotal}	Total pressure coefficient
$C_{Pstatic}$	Static pressure coefficient
P	Pressure sensed by different holes
α	Pitch angle (°)
β	Yaw angle (°)
ρ	Density (kg/m^3)
ρ_m	Density of manometric fluid (kg/m^3)
ρ_{air}	Density of air (kg/m^3)
Subscripts	Hole numbers
1, 2, 3, 4, 5, 6, 7	
I	i^{th} data point in a given sector
°	Degree
Superscripts	Average
¯	

I. INTRODUCTION

The seven-hole probe is a pressure measuring device as, having the capability of providing quantitative information about the three components of flow velocity as well as about the total and dynamic pressure. The popularity of the seven-hole probe came into being due to the inaccurate measurement of the five-hole probe and hot wire probe when local pitch and yaw angles exceed ±30º.

The application of seven-hole probe was developed to measure flow angularity which is better senility than five hole pressure probe. Development of the seven-hole probe, the calibration technique and interpolation procedure is described by Gallinton [1]. It involved positioning the probe at known angles to the flow and then measuring the seven pressures. A sectoring scheme is applied to choose to find the flow properties based on the highest pressure sensed by each port. Third order polynomial functions for the flow properties are then determined based on the pressure coefficients and the probe inclination. The calibration approach developed by Gallinton is unique and quite ingenious.

Everett et.al [2] made some improvements by simplifying in the calibration technique and increasing its accuracy. The third order polynomial expression used to determine the flow properties are based on minimum 20 calibration points and a 5º increment between the points. The limit ranged to

±65º at Mach 0.88 and ±85º at Mach 0.20, although the variation of Reynolds number revealed no significant role on the calibration coefficients. There are a number of different approaches to the aforementioned procedure, varying in the definitions of the pressure coefficients and the method of curve fitting. Using only one set of coefficient definitions limits the angular range the probe can resolve since at high incidence angles the flow over one or more of the ports may be separated. Gerner and Maurer [3], Gerner and Sisson [4], used seven-hole probes and split the angular domain into low-angle and high-angle flows similar to the methods by Bryer and Pankhust, and extended the usable angular range up to 70º in cone angle (angle between the velocity vector and the probe axis). Gerner and Maurer [3] defined separate non-dimensional pressure coefficients for the pitch and yaw angles. These coefficients were designed to be sensitive primarily to one of the two angles and not to the other. In other words, each one has a linear dependence on their respective angle and independence to the other angle. Also, like all pressure coefficients, these too are dependent upon Mach number and this becomes apparent only in the compressible regime (M > 0.3). As a corollary, the calibration data from any Mach < 0.3 can be used for the entire incompressible regime. The polynomial fitting of the non-dimensional coefficients to the flow angles has been studied extensively. Most early work used either a global procedure, where polynomials were created for all calibration points, or a sector based procedure (Gerner and Maurer) [3]). Rediniotis et al. [5] were able to increase accuracy by dividing the port specific regions into several sections, thereby increasing the number of regions for which polynomials were need to describe the calibration coefficients. Zilliac [6] developed methods that are local in nature, where a calibration database is searched and interpolation or curve-fitting is performed locally, using only a few data points.

Zilliac [6] used the akima interpolation method [7], which is a weighted-nearest-neighbours method, instead of the more common (equally-weighted) curve-fit method and found significant reduction in errors. He also devised a simple technique to identify (and evade) pressure ports in the separated region of the seven-hole probe. Rediniotis and Vijayagopal [8] used Artificial Neutral-Networks (ANN) rather than traditional polynomial fitting to relate the coefficient to the flow angles and found good prediction capabilities. Clark et al. [9] calibrated hemispherical tipped probes in high subsonic up to Mach 2.0 flows, examining five different calibration coefficient definitions for number effects. They also compared ten identically produced probes and found that individual calibrations were required for each single probe due to manufacturing idiosyncrasies. Takahashi [10] performed analysis on the coefficient behavior identifying also optimizing for processing speed. The maximum flow incidence angle that can be resolved by a five-hole or seven-hole probe depends on the probe tip geometry and port locations. Most probes can accurately resolve angles up to approximately 70º. Gregory H. Johnson and Lawrence S. Reed [11] studied the seen-hole probe in the shear flow in order to help correct measurements in the presence of shear flow. The interpolation scheme involved to back step from apparent flow by the use of measurement obtained by the probe. It permitted manual corrections of erroneous apparent flow angles and establishes the foundation for surface fit shear gradient corrections. C. Venkateswara Babu et. al [12] developed a hybrid methods combining the polynomial curve fit and the direct interpolation method for the seven-hole probe. They calibrated the seven-hole probe in the range of ±50º at 9º interval and divided the probe in seven zones. The calibrations coefficients are derived for each zone depending on the maximum pressure sensed. A localized two variable polynomial is used at each point with the data surrounding it. The interpolation errors in flow angles were found to be within ±1º and the errors in the total and static pressure are within 0.5% and 1% of the dynamic pressure. M.C. Gamerio Silva et. al [13] compared the conventional method of interpolation to their direct interpolation method. Their method uses a linear interpolation directly performed on the dimensional coefficients matrices that were generated during the calibration procedure. They also conclude the direct interpolation has better accuracy and result uniformity than the conventional procedure. Espen S. Johansen, Rediniotis [14] developed a data reduction algorithm for non-nulling multi-hole pressure probes suitable for both five-hole and seven-hole probes. Their method was also accurate for ±0.6º for flow angles and velocity is predicted within ±1% as documented in the literature. Arnoud R.C. Franken and Paul C. Ivey [15] used four-hole cobra probe and four-hole pyramid probe and tried the rational function interpolation method, polynomial curve-fit method and the neural network for the data reduction technique. Although they stressed on the neural network but hadn't specified any comparison between the techniques. Mathew D. Zeiger and Norman W. Schaeffler [16] presumed a computational method to determine the alignment bias angles for the multi-hole straight probes. The method also determined the vertical bias angles, which cannot be determined experimentally in cone-

roll coordinates. A comparison between the computational method and the traditional method yielded a difference of 0.16º. A. J. Pisascale and N. A. Ahmed [18] developed a functional relationship best on theoretical Considerations (potential flow), which related the port pressures directly as the flow properties. The relationship resulted in determining large flow angles to accuracy better than 0.8º. David Sumner [18] compared the data reduction techniques provided by Gallinton [1] and Zilliac [5] for the calibration of a seven-hole conical pressure probe in an incompressible flow. The data reduction techniques were both applied to same set of calibration data and it was found at low flow angles (less than 30º) where the flow remain attached to the probes both the methods yielded competitive results for an interval of maximum 10º. The direct interpolation method of Zilliac had an advantage over Gallington's method only when flow angle exceeds 30º. He also concluded that the probe effectiveness gets reduced when Reynolds number exceeds 5000. For many complex flow-fields, the angular range in the measurement domain (either spatially, temporally, or both) is greater than what a five-hole or seven-hole probe can resolve (the flow in the wake of a bluff body), and for such flows the omni-directional probe can be used. The omni probe is an extension of the five-hole and seven-hole probes with the distinct advantage that it can resolve flow angles up to 160º from its principal axis. Similar to the five-hole probe, the omni probe predict the flow angles, the local total and static pressures, and the velocity magnitude with a high degree of accuracy.

II. EXPERIMENTAL SET UP AND ALGORITHM FOR NON- NULL METHOD WITH SECTOR SCHEME

Schematic diagram of the experimental set up used for this study is shown in Fig.1. The main components of the experimental set up include an air supply unit, flow control arrangement, settling chamber, contraction cone and a straight test section. Every component, except the air supply unit and the straight test section were made of wood. The straight test section was made of transparent plexiglass. However, calibration is done in the open jet of air coming out from the test section. Ambient air is used as flowing fluid during calibration.

A hemispherical tip seven-hole pressure probe as shown in Fig.2(c), has been used for the calibration. It consists of seven stainless steel tubes of outer diameter 1.2 mm and inner diameter of 0.9 mm glued together. The tubes are then put into a jacket tube of 4.16 mm diameter. The short L-shape tip was thin, filled with the molten solder. The tip was filled to give the shape of the hemisphere. Seven holes on the face of the hemispherical tip are fixed in such a manner so that one hole being at the center and the remaining six holes are mutually apart with each other forming an angle of 45º with respect to the center hole. The probe was 'L' shaped with the length of 'L' being 4 mm. Due to this length, the effect of blockage at the point of measurement is significantly reduced, (less than 3%). The length of the seven-hole pressure probe is 0.27 m.

The central hole 1 measures the reference pressure, which is the stagnation pressure when the probe is at 0º yaw. The change in pressures across the two horizontal holes marked 3 and 5 are used to calculate the flow direction in the horizontal plane, the yaw angle, while the pressure change across the two vertical holes 1 and 4 are related to a change in pitch angle. The pressure on the central tube is generally the largest of the seven pressures (depending upon the flow angles).

The principle is easiest to understand when looking at the individual changes in orientation, i.e. only horizontal change (yaw only) or only vertical change (pitch only). In order to limit the length of this section, only the pressure variations for a decreasing yaw angle and zero pitch will be described. The pressure changes for the orientations are shown in Table (3.4) and should be easily derived from the example given below. If the probe is rotated to -veº yaw and +veº pitch angle then hole 2 is oriented more perpendicularly to the flow and therefore is a larger obstacle in the flow. This results in a lower velocity across the face and a higher the pressure on the face hole 2. The velocity of the flow over the hole 6 is higher hence the pressure drops in hole - 6. As a result the pressure difference across (P2 – P6) increases and vice-versa.

If the yaw angle between the flow direction and the probe were increased even further to negative degrees yaw, hole 2 would read stagnation pressure, while hole 6 would read static pressure. However if separation of the flow occurs at the edge, a separation bubble can occur, which leads to highly fluctuating pressure readings in hole 6.

The seven-hole probe calibration technique involves positioning the probe at known angle to the flow and then measuring the seven pressures. Dimensionless velocity-invariant pressure coefficients, based on combination of differences between the seven measured pressures are formed. A sectoring scheme as shown in Fig.3(b) is used to choose certain combinations of the pressure coefficients depending on the relative magnitude of the seven measured pressures. This sectoring approach permits the measurement of flows of high angularity selecting the highest pressure sensed by a hole. However, the compressibility effects were

neglected as flow speed was limited to 40m/s. But, the calibration technique can be extended to compressibility regime by introducing a dimensionless compressible term in the calibration equation Everett et.al [33]. The calibration is carried out in two phases, for low angles (maximum centre hole pressure) and high angles (outer periphery holes sensing maximum pressure).

4.31 Low Angles

In case of low flow angles when the maximum pressure is sensed by the centre hole, flow remains attached over the all seven holes i.e. no stalling occurs. Therefore all the seven pressures are used to define the angular pressure coefficients which vary linearly with the flow angles. The three dimensionless pressure coefficients are defined as follows:

$$C_{P\alpha} = (P_4 - P_1) \Big/ (P_7 - P))$$

$$C_{Pb} = (P_5 - P_2) \Big/ (P_7 - P)$$

$$C_{Pc} = (P_6 - P_3) \Big/ (P_7 - P)$$

$$\overline{P} = (P_1 + P_2 + P_3 + P_4 + P_5 + P_6) / 6$$

Only two of these three coefficients are needed to specify the orientation of an oncoming velocity vector uniquely arbitrarily selecting a pair of coefficients eliminates the additional pressure information available to the third coefficient. So the equations are taken and resolved into a single pair of pitch and yaw reference system.

$$C_{P\alpha} = (2C_{pa} + C_{pb} - Cp_{pc}) \Big/ \sqrt{3}$$

$$C_{P\beta} = (2C_{pb} + C_{pb} - Cp_{pc}) \Big/ 3$$

$$C_{PT} = (P_7 - P_T) \Big/ P_T - Ps)$$

$$C_{PS} = (P_S - \overline{P}) \Big/ (P_T - P_S)$$

When flow angle exceed 30º (depends on the probe geometry and manufacturing accuracies) the flow on the lee side (downstream portion of the probe) tends to separate. Since the probe tip is hemispherical in shape separation normally occurs between 90º and 100º (Zilliac [6]). The probe tip receives a forward velocity component which attaches only to four holes out of seven holes. The remaining holes lie in the separated region and are stalled. Therefore the pressure coefficients are defined on the basis of the response of the four holes which lie in the attached flow. A total of twelve dimensionless pressure coefficients are formed for use of high flow angles (greater than approximately 20º) as described by Gallington [1].

Pressure coefficient for sector 1

SECTOR 1

$$C_{P\alpha 1} = (P_1 - P_7) \Big/ P_1 - (P_2 + P_6 / 2)$$

$$C_{P\beta 1} = (P_6 - P_2) \Big/ P_1 - (P_2 + P_6 / 2)$$

$$C_{PT1} = (P_1 - P_T) \Big/ P_1 - (P_2 + P_6 / 2)$$

$$_{PS1} = (P_2 + P_6)/2 - P_S \Big/ P_1 - (P_2 + P_6 / 2)$$

Pressure coefficient for sector 2

SECTOR 2

$$C_{P\alpha_2} = (P_2 - P_7) \Big/ P_2 - (P_1 + P_3 / 2)$$

$$_{P\beta_2} = (P_1 - P_3) \Big/ P_2 - (P_1 + P_3 / 2)$$

$$_{PT_2} = (P_2 - P_T) \Big/ P_2 - (P_1 + P_3 / 2)$$

$$_{PS_2} = (P_1 + P_3)/2 - P_S \Big/ P_2 - (P_1 + P_3 / 2)$$

Pressure coefficient for sector 3

SECTOR 3

$$C_{P\alpha_3} = (P_3 - P_7) \Big/ P_3 - (P_2 + P_4 / 2)$$

$$_{P\beta_3} = (P_2 - P_4) \Big/ P_3 - (P_2 + P_4 / 2)$$

$$_{PT_3} = (P_3 - P_T) \Big/ P_3 - (P_2 + P_4 / 2)$$

$$_{PS_3} = (P_2 + P_4)/2 - P_S \Big/ P_3 - (P_2 + P_4 / 2)$$

Pressure coefficient for sector 4

SECTOR 4

$$C_{P\alpha_4} = \frac{(P_4 - P_7)}{P_4 - (P_3 + P_5/2)}$$

$$P\beta_4 = \frac{(P_3 - P_5)}{P_4 - (P_3 + P_5/2)}$$

$$PT_4 = \frac{(P_4 - P_T)}{P_4 - (P_3 + P_5/2)}$$

$$PS_4 = \frac{(P_3 + P_5)/2 - P_S}{P_4 - (P_3 + P_5/2)}$$

Pressure coefficient for sector 5

SECTOR 5

$$C_{P\alpha_5} = \frac{(P_5 - P_7)}{P_5 - (P_4 + P_6/2)}$$

$$P\beta_5 = \frac{(P_4 - P_6)}{P_5 - (P_4 + P_6/2)}$$

$$PT_5 = \frac{(P_5 - P_T)}{P_5 - (P_4 + P_6/2)}$$

$$PS_5 = \frac{(P_4 + P_6)/2 - P_S}{P_5 - (P_4 + P_6/2)}$$

Pressure coefficient for sector 6

SECTOR 6

$$C_{P\alpha_6} = \frac{(P_6 - P_7)}{P_6 - (P_5 + P_1/2)}$$

$$P\beta_6 = \frac{(P_5 - P_1)}{P_6 - (P_5 + P_1/2)}$$

$$PT_6 = \frac{(P_6 - P_T)}{P_6 - (P_5 + P_1/2)}$$

$$PS_6 = \frac{(P_5 + P_1)/2 - P_S}{P_6 - (P_5 + P_1/2)}$$

4.33 Interpolation Procedure:

The interpolation method uses $C_{P\alpha}$ and $C_{P\beta}$ as independent variables in deriving a localized polynomial to calculate the dependent variables such as pitch angle (a). yaw angle total pressure (P_T) and static pressure (Ps). At each calculating point of the elected zone, the interpolation chooses a polynomial locally by using the calibrated data surrounding it. Four different response equations is found for each sector, one four each of the four flow properties.

(α, β, C_{PT}, C_{PS},). Each flow property is represented by a fourth order polynomial expansion of the pressure coefficient ($C_{P\alpha}$ and $C_{P\beta}$). Using all of the calibration data within a sector, a least squares technique is used to find the polynomial coefficients, K_1 to K_{15}, for each flow property and sector combination. Therefore a total number of 28 polynomials functions and 42 calibration constant are derived. The four flow properties are defined as follows:

$$\alpha_i = K_1,\alpha_i + K_2,\alpha_i \times C_{p\alpha,i} + K_3,\alpha_i \times C_{p\beta,i} + K_4,\alpha_i \times C^2_{p\alpha,i} + K_5,\alpha_i \times C_{p\alpha,i} \times C_{p\beta,i} + K_6,\alpha_i \times C^2_{p\beta,i} + K_7,\alpha_i \times C^3_{p\alpha,i} + K_8,\alpha_i \times C^2_{p\alpha,i} \times C_{p\beta} + K_9,\alpha_i \times C_{p\alpha,i} \times C^2_{p\beta,i} + K_{10},\alpha_i \times C^3_{p\beta,i} + K_{11}\alpha_i \times C^4_{p\alpha,i} + K_{12},\alpha_i \times C^3_{p\alpha,i} \times C_{p\beta,i} + K_{13},\alpha_i \times C^2_{p\alpha,i} \times C^2_{p\beta,i} + K_{14},\alpha_i \times C_{p\alpha,i} \times C^3_{p\beta,i} + K_{15},\alpha_i \times C^4_{p\beta,i} \quad \ldots (1)$$

$$\beta_i = K_{1,\beta i} + K_{2,\beta i} \times C_{p\alpha,i} + K_{3,\beta i} \times C_{p\beta,i} + K_{4,\beta i} \times C^2_{p\alpha,i} + K_{5,\beta i} \times C_{p\alpha,i} \times C_{p\beta,i} + K_{6,\beta i} \times C^2_{p\beta,i} + K_{7,\beta i} \times C^3_{p\alpha,i} + K_{8,\beta i} \times C^2_{p\alpha,i} \times C_{p\beta,i} + K_{9,\beta i} \times C_{p\alpha,i} \times C^2_{p\beta,i} + K_{10,\beta i} \times C^3_{p\beta,i} + K_{11,\beta i} \times C^4_{p\alpha,i} + K_{12,\beta} \times C^3_{p\alpha,i} \times C_{p\beta,i} + K_{13,\beta i} \times C^2_{p\alpha,i} \times C^2_{p\beta,i} + K_{14,\beta i} \times C_{p\alpha,i} \times C^3_{p\beta,i} + K_{15,\beta i} \times C^4_{p\beta,i} \quad \ldots\ldots\ldots\ldots\ldots\ldots (2)$$

$$C_{pSi} = K_{1,Si} + K_{2,Si} \times C_{p\alpha,I} + K_{3,Si} \times C_{p\beta,i} + K_{4,Si} \times C^2_{p\alpha,i} + K_{5\,Si} \times C_{p\alpha,i} \times C_{p\beta,i} + K_{6,Si} \times C^2_{p\beta,i} + K_{7,Si} \times C^3_{p\alpha,i} + K_{8,Si} \times C^2_{p\alpha,i} \times C_{p\beta,i} + K_{9,Si} \times C_{p\alpha,i} \times C^2_{p\beta,i} + K_{10,Si} \times C^3_{p\beta,i} + K_{11,Si} \times C^4_{p\alpha,i} + K_{12,Si} \times C^3_{p\alpha,i} \times C_{p\beta,i} + K_{13,Si} \times C^2_{p\alpha,i} \times C^2_{p\beta,i} + K_{14\,Si} \times C_{p\alpha,i} \times C^3_{p\beta,i} + K_{15,Si} \times C^4_{p\beta,i} \quad \ldots\ldots\ldots (3)$$

$$C_{pTi} = K_{1,Ti} + K_{2,Ti} \times C_{p\alpha,i} + K_{3,Ti} \times C_{p\beta,i} + K_{4,Ti} \times C^2_{p\alpha,i} + K_{5,Ti} \times C_{p\alpha,i} \times C_{p\beta,i} + K_{6,Ti} \times C^2_{p\beta,i} + K_{7,Ti} \times C^3_{p\alpha,i} + K_{8,Ti} \times C^2_{p\alpha,i} \times C_{p\beta,i} + K_{9,Ti} \times C_{p\alpha,i} \times C^2_{p\beta,i} + K_{10,Ti} \times C^3_{p\beta,i} + K_{11,Ti} \times C^4_{p\alpha,i} + K_{12,Ti} \times C^3_{p\alpha,i} \times C_{p\beta,i} + K_{13,Ti} \times C^2_{p\alpha,i} \times C^2_{p\beta,i} + K_{14,Ti} \times C_{p\alpha,i} \times C^3_{p\beta,i} + K_{15,Ti} \times C^4_{p\beta.i} \quad \ldots\ldots\ldots (4)$$

Where, the superscript i depends on the sector chosen i.e. i = 1 to 7.

The final step is to determine the velocity components in three directions as shown in Fig.3(a) which can be found from the following equations.

$$\overline{U} = \sqrt{(P_T - P_S) \times (\rho_m \times g \times 2/\rho_{air})}$$

$$\underline{U}_x = \overline{U} \times \cos\alpha \times \cos\beta$$

$$U_y = \overline{U} \times \sin\beta$$

$$U_z = \overline{U} \times \sin\alpha \times \cos\beta$$

A hemispherical tip seven-hole pressure probe as shown in Fig.2 has been used for the calibration. It consists of seven stainless steel tubes of outer diameter 1.2mm and inner diameter of 0.9mm glued together. The length of the seven-hole pressure probe is 0.27m. A probe traversing gear has been

designed for the present study, which allows the rotation of the probe in both pitch and yaw plane [20].

A simple regression method of matrix terms as discussed by Netter and Washerman [19] has been used in the present study for determining the different calibration coefficients as required.

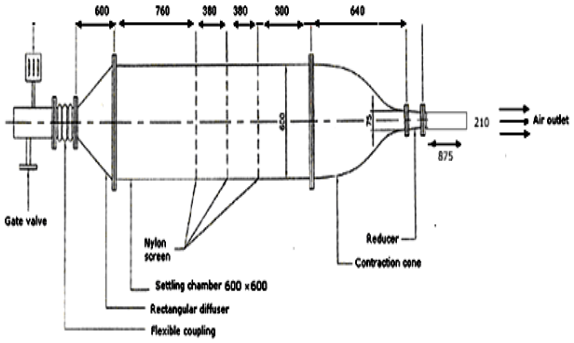

Fig.1. Schematic diagram of experimental setup

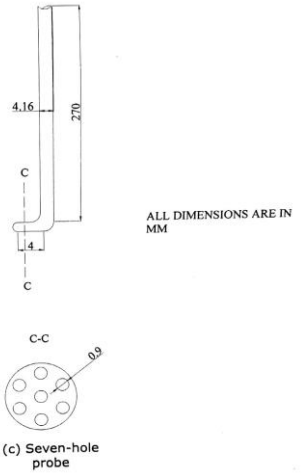

Fig.2. Schematic diagram of the pressure probe

The sector method divides the entire calibration zone into seven parts, one central zone and six side zones .The zones are chosen based on the highest pressure sensed by the holes e.g. when center hole senses maximum pressure, zone 1 is taken. Detailed view of the probe with zonal discrimination is given in Fig. 3(a-b).

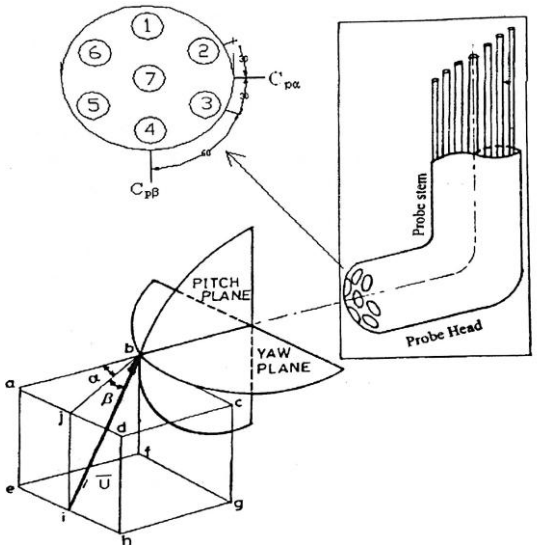

(a) Section view with hole nomenclature

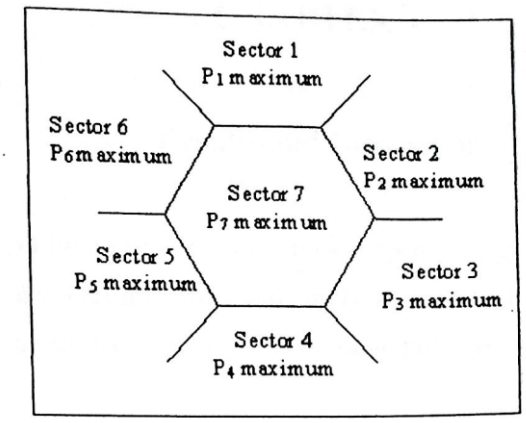

(b) Different sectors chosen

Fig.3. Sectoring scheme chosen for seven-hole probe
(hole numbers 1to 7)

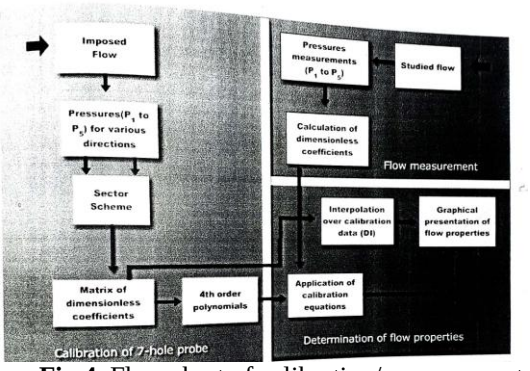

Fig.4. Flow chart of calibration/measurement process by
Seven-hole probe

$$\overline{U} = \sqrt{(P_T - P_S) \times (\rho_m \times g \times 2/\rho_{air})}$$

$$U_x = \overline{U} \times \cos\alpha \times \cos\beta$$

$$U_y = \overline{U} \times \sin\beta$$

$$U_z = \overline{U} \times \sin\alpha \times \cos\beta$$

III. RESULTS AND DISCUSSIONS

Here the calibration curves of the flow properties (e.g. pitch angle, yaw angle, static pressure and total pressure) for a seven-hole probe (non-null technique) obtained by are discussed.

A flowchart is provided for understanding of the various processes involved for the measurement of flow properties with seven-hole probe. The interpolation techniques of the seven-hole probe with respect to the flow properties obtained by interpolation are compared with measured flow properties to gain a better view of the error.

The seven-hole probe calibration technique is based on the sector approach which has a distinct advantage by extending the angular range of the probe where the flow is Reynolds number invariant. In the case of the five-hole probe calibrating over the entire calibration data cannot be possible for the seven-hole probe because the calibration coefficient based on the pressure variation sensed by the holes located beneath the separated region will no longer uniquely determine the flow angles. A flowchart considering the two ays (4OP and DI) of using the seven-hole directional pressure with non-nulling methods for the assessment of the flow characteristics is presented in Fig.4.

Fig.6. is the α-β map of sectors chosen by the calibration scheme. The symbols indicate the holes registering the maximum pressure. The nomenclature indicating the hole names are derived by considering the probe facing the flow. From the figure it is clearly visible that for a certain range of α and β, a particular hole will sense the maximum pressure. This theory was utilized for deriving the calibration constants. The calibration pressure was divided into two parts low angle and high angle. At low angle centre zone was chosen and at high angle the other zones were chosen. The word "flow separation" repeatedly used that text now can be easily understood by visualization of the figures. When the out periphery holes senses the maximum pressure the flow is said to be separated.

The contour of α versus β shown in Fig.5(a) to Fig. 5(g) indicate the variation of pressure in the seven-hole probe for each pressure holes (P_1-P_T) within the sectors they lay. The contours shows arcs of increasing pressure depending on the flow angles (α and β) ascending or descending.

Fig.5(a) shows the contours of α versus β with the variation of pressure in hole1. It gives a better understanding of the high angle flow as the side hole senses maximum pressure when the probe is oriented at an angle α = 35º and β lies between -5º to +5º. It is clearly visible when the curvature of the arc increases the pressure increases and the velocity accordingly hole decreases.

Fig.5(b) shows the contours of α versus β with the variation of pressure in hole 2 when it sense maximum pressure with respect to the other holes. The arcs are non-symmetric in nature due to geometrical inaccuracies in manufacturing. The maximum pressures senses by hole 2 when the probe is oriented to the flow at an angle, β = -30º and α > 0º.

Fig.5(c) shows the contours of α versus β for which maximum pressure sensed by hole 3 with respect to other holes, corresponding to the mean velocity of flow. Pressure in hole 3 becomes maximum when the probe is oriented to the flow at an angle when a lies between 25º to -30º and β ≥ -30º. At α = -28º and β = -30º P_3 senses stagnation pressure and velocity across the hole becomes minimum.

Fig.5(d) shows the contours of α versus β for which maximum pressures sensed by hole – 4 with respect to other holes, corresponding to the mean velocity of flow. It represents the change of pressure in hole 4 with the change in α and β. The maximum pressure sensed by hole 4 when a lies within -10º to +15º and β -20º to -30º. The hole 4 will read stagnation pressure when the probe is oriented at an angle α = -5º and β = -30º towards the flow.

Fig.5(e) shows the contours of α versus β for which maximum pressures sensed by hole 5 with respect to other holes, corresponding to the mean velocity of flow. It represents the change of pressure in hole 5 with the change in α and β. The maximum pressure sensed by

hole 5 when a lies within +12º to +30º and β -30º to -8º. The hole 5 will read stagnation pressure when the probe is oriented at an angle α = 25º and β = 27º towards the flow.

Fig.5(f) shows that the contours of α versus β for which maximum pressures sensed by hole 6 with respect to other holes, corresponding to the mean velocity of flow. It represents the change of pressure in hole 6 with the change in α and β. The maximum pressure sensed by P6 when a lies within -5º to +35º and β -30º to -20º. The hole 6 will read stagnation pressure when the probe is oriented at an angle α = 10º and β = -25º towards the flow.

Fig.5(g) shows the contours of α versus β for which maximum pressures sensed by hole 7 with respect to other holes, corresponding to the mean velocity of

flow. It is the central zone of the probe and maximum pressure occurs at lo angles with the change in α and β. The maximum pressure sensed by hole 7 when a lies within -20º to +15º and β -20º to +15º. The hole 7 will read stagnation pressure when the probe is oriented at an angle α = -5º and β = 0º towards the flow. However, theoretically this should occur at α = 0º and β = 0º, but manufacturing defects effects probe symmetry resulting in the above distortion.

The Fig.5(a) to Fig.5(f) shows the variation of yaw angle coefficient (C_{pyaw}) versus pitch angle coefficient (C_{ppitch}) for each sector. These figures demonstrate that a is primarily dependent on C_{ppitch} and β is primarily dependent on C_{pyaw}. As discussed earlier Zone (1-6) denotes high flow angles but these data are such that they are unique values for a and β for any combination of C_{pyaw} and C_{ppitch}. The variations shown in the curve are used to interpolate the flow angles α and β when the probe is used for field measurement. It can also be deduced from the curves that for high flow angles the spacing between the C_{pyaw} and C_{ppitch} is least as compared to low angle (centre zone). The variation of C_{pyaw} to C_{ppitch} for the centre zone (hole 7) is similar to the behavior observed by the centre hole of the five hole probe discussed in previous section. The Fig. 5(a) to Fig.5(d) shows the variation of yaw angle versus C_{ptotal} for different pitch angles for zone 1, zone 2, zone 3 and zone 4. Fig.5(a) to Fig.5(d) shows the variation of yaw angle versus Cpstatic for different pitch angles for zone 1, zone 2, zone 3 and zone 4. The two calibrations

curves C_{ptotal} and $C_{pstatic}$ can be determined by interpolation over a and β. But this leads to errors as both a and β are determined from interpolation and are error carriers for next interpolation. Therefore yaw angle coefficient and pitch angle coefficient are used to interpolate the values of $C_{pstatic}$ and C_{ptotal} as discussed in Chapter IV.

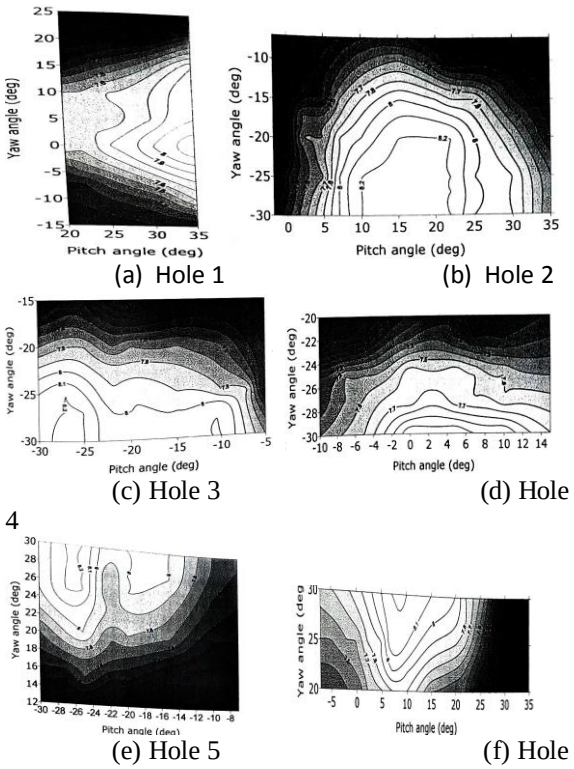

(a) Hole 1 (b) Hole 2

(c) Hole 3 (d) Hole 4

(e) Hole 5 (f) Hole 6

(g) Hole 7

Fig.5. Pressure hole of Seven-hole probe response to pitch and yaw angle.

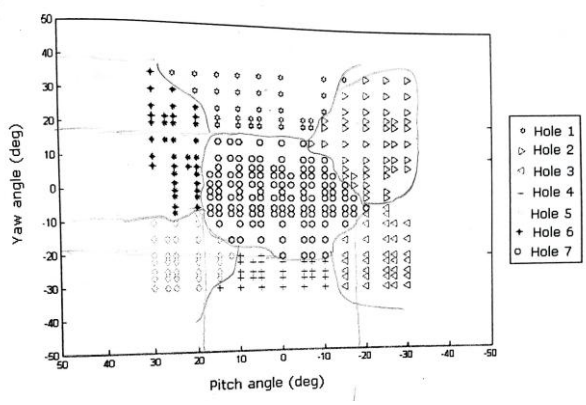

Fig.6. Sector map of pitch and yaw angle of seven-hole probe

Error:

To allow the assessment of errors resulting from the 4th order polynomial and direct interpolation method, data about flows with directions corresponding to intermediate points in the two grids of angles were acquired during the calibration procedure. For those flows, which data was not included in the matrices resulting from the calibration, the characteristic were calculated using the aforementioned methods, where the pressure measured in the probe seven holes were the input data. Once the flow characteristics were imposed and thus, known in advance, it is possible to compute the error method, subtracting the calculated values from the imposed ones.

It is possible to obtain maps with the distribution of the errors as a function of the entire incidence angles for each of the flow characteristic in all the probe sectors.

A comparison between the 4th order polynomial and direct interpolation method can be analyzed. The error to pitch angle, yaw angle, static pressure coefficient and total pressure coefficient with the measured value is depicted for the centre zone (hole 7) and one periphery zone (hole 2). The comparison of error assessment of the two zones by the two interpolation methods for the pitch angle and yaw angle. Considering the direct interpolation scheme and the 4th order polynomial interpolation for zone 7 and zone 2 sector are comparative to each other. In zone 7 interpolation of pitch angle, the D.I. (direct interpolation) has better accuracy than the 4OP method, except some cases e.g. (4OP interpolated result of β at -15º, α at -10º was better than DT). In zone 2, result for a and β clearly states that the DT method has got an advantage over 4OT. The errors in the pressure coefficients are though very small (in the order of .01) for both the methods, but 4OP generates better result against DI in some cases. In general both the methods can be used for interpolation, but the 4OP is time consuming as separate Fortan code is to be generated but the DI with the help of Matlab 7.0 interpolation directly from the calibration data and is ls tedious.

IV. Conclusion

The following conclusions are made based on the present study:

1. The seven-hole probe calibration technique is based on the sector approach which has a distinct advantage by extending the angular range of the probe where the flow is Reynolds number invariant.
2. Among the two data reduction technique used, direct interpolation method showed supremacy over the 4th order polynomial method. The data reduction technique yielded an accuracy of ±1° both in pitch and angle and ±1.5 m/s in velocity.
3. The interpolation techniques of the seven-hole probe with respect to the flow properties obtained by interpolation are compared with measured flow properties to gain a better view of the error.

REFERENCES

[1]. Gallington R.W., "Measurement of very large flow angles with non-nulling seven-hole probes". *Aeronautic Digest* Spring/Summer (USAF Academy), 1980

[2]. Everest, K.N., Gerner, A.A., and Durston, D.A., 1982, "Theory and Calibration of Non- Nulling Seven-Hole Cone Probes for use in Complex Flow Measurement." AIAA paper 820232, AIAA *20th Aerospace Sciences Meeting*, Orlando, Jan.

[3]. Gerner, A.A. and Maurer, C.L., 1981, "Calibration of Seven-Hole Probe Suitable for High Angles in Subsonic Compressible Flows," United States Air Force Academy-TR-81-4.

[4]. Germer, A.A, and Sisson, G., 1981, "Seven-Hole Probe Data Acquisition System" United States Air Force Academy-TN-81-8, Nov.

[5]. Rediniotis, O.K. and Pathak, M.M. 1999, "Simple Technique for Frequency-Response Enhancement of Miniature Pressure Probes." AIAAJ, 37, no.7, PP. 897-899

[6]. Zilliac, G.G., 1989, "Calibration of Seven-Hole Probe for Ue in Fluid Flows with Large Angularity, " NASA Technical Memorandum 102200, Dec.

[7]. H. Akima, A method of bivariate interpolation and smooth surface fitting for irregularly distributed points, ACM Transactions on Mathematical Software 2 (4) (1978) 148.

[8]. Rediniotis OK, Vijayagopal R., (1999) Miniature multi-hole pressure probes and their neural-network-based calibration. AIAAI 37:666-674.

[9]. Clark, E.L., Henfling, J.F., and Aeschlimqn, D.P., 1992, "Calibration of Hemispherical-Head Flow Angularity Probes," AIAA Paper 92-4005, AIAA *17th Aerospace Ground Testing Conference*, Nashville, July.

[10]. Takahashi, T.T., 1997, "Measurement of Air Flow Characteristics Using Seven-Hole

Cone Probes," NASA Technical Memorandum 112194, May.
[11]. Johnson G.H and Lawrence S.R., "Seven-hole probe in shear flow" American Institute of Aeronautics and Astronautics.
[12]. Babu, Venkatewara, C, Govardhan M, and Sitaram, N, 1998, "A method of calibration of a seven-hole pressure probe for measuring highly three dimensional flows," Meas. Sei. Feehnol., 9, pp. 468 – 476.
[13]. M.C.G. Silva, A.M.O. Lopes, C.A.C. Pereira, J.M.S. Cruz, "On the use of a linear interpolation method in the measurement procedure of a seven-hole pressure probe", Experimental Thermal and Fluid Science 28 (2003) 1 – 8.
[14]. Johonsen, E.S., Rediniotis, O.K., and Jones, G. 2001, "The Compressible Calibration of Miniature Multi-Hole Probes," ASME J, of Fluids Engineering, 123. Pp. 128-138.
[15]. Arnoud R.C. Franken and Paul C. Ivey, "Accelerating the Calibration of Multihole Pressure Probes by Applying Advanced Computational Methods", International Gas Turbine and Aero-engine Congress and Exhibition, Vienna, Austria, June 13 – 17, 2004, Paper No. 2004-GT-53434.
[16]. D.Z. Mathew and W.S. Norman, "Correcting multi-hole probe alignment bias errors post-calibration", American Institute of Aeronautics and Astronautics, 2001.
[17]. Pisasale A. J. Ahmed N.A., "Development of a functional relationship between post-pressures and flow properties for the calibration and application of multi-hole probes to highly three-dimensional flows". Experiment of Fluids 36 (2004) 422 – 436.
[18]. Summer D, "A Comparison of Data-Reduction Method for a Seven-Hole Probes, the Journal of Fluids Engineering November 21, 2001.
[19]. Netter.J and Washerman.W, "Simple regression model in matrix terms", Applied linear Statistical Models, Richard D.Irwin, Inc, III,pp 200, 1975.
[20]. Chowdhury, D., "Modeling and calibration of pressure probes",M.P.E. Thesis, Jadavpur University, 2007